Effects of Adsorbent Conductivity and Permeability on the Performance of a Solid Sorption Heat Pump

M. W. Ellis
Department of Mechanical Engineering,
Virginia Polytechnic Institute
and State University,
Blacksburg, VA 24061-0238

W. J. Wepfer
The George W. Woodruff School of
Mechanical Engineering,
Georgia Institute of Technology,
Atlanta, GA 30332-0405

Solid sorption heat pumps can improve the effectiveness with which energy resources are used for heating and cooling. These systems operate by alternately heating and cooling beds of adsorbent material to produce a flow of refrigerant. The research presented here evaluates the effects of adsorbent thermal conductivity and permeability on the performance of a thermal wave solid sorption heat pump. In order to evaluate these effects, a numerical model of the thermal wave heat pump is developed. This model incorporates not only the effects of the conductivity and permeability, but also the effects of the adsorption equilibrium properties, refrigerant properties, application parameters, operating parameters, and bed geometry. For a typical air conditioning application, the model is used to study the influence of conductivity and permeability on the COP for systems using ammonia as a refrigerant. The results indicate that for the geometry considered, increasing the thermal conductivity of the adsorbent to 1 W/m-K can improve the COP to approximately 0.75. Further increases in conductivity do not yield improved performance. Furthermore, the reduced permeability associated with high conductivity adsorbents can impair vapor flow and lead to decreased performance.

Introduction

Thermally driven heat pumps can reduce the impact of growing global energy demands by improving the efficiency with which fossil fuel resources are used. Thermally driven heat pumps use the thermal energy produced by combustion to directly operate the heat pump cycle. Thus, they eliminate the generation and transmission losses associated with traditional electric heat pumps. The ability to operate a heat pump using thermal energy also provides industry with better opportunities for the recovery of waste heat.

The solid sorption heat pump cycle is one of the more promising thermally driven heat pump cycles. Solid sorption cycles can provide high performance, simple operation, and wide operating temperature ranges. A variety of research and development is currently underway to improve the performance of these cycles and to make them commercially viable. This article investigates the feasibility of using adsorbent materials with enhanced thermal properties to improve the performance of a particular type of solid sorption cycle known as the thermal wave cycle.

The thermal wave cycle has been described by Shelton (1986) and by Tchernev (1987). The system is illustrated in Fig. 1. The equipment includes two adsorbent heat exchangers, each consisting of tubes embedded in adsorbent material. Fluid circulating through the tubes heats or cools the adsorbent material. The heated adsorbent material in Bed A desorbs refrigerant at a relatively high pressure. The refrigerant leaving Bed A is condensed, expanded, and evaporated, and then adsorbed into the material in Bed B. This requires cooling Bed B to remove the heat released by the adsorbing refrigerant. Periodically, as Bed A is exhausted (and Bed B is saturated), the roles of the two beds are reversed.

A portion of the energy removed from Bed B can be used to heat Bed A. This is called regeneration and can significantly improve the cycle efficiency. In the thermal wave cycle, regeneration is accomplished by designing the adsorbent heat exchangers to yield steep thermal gradients along the direction of heat transfer fluid flow. As illustrated in Fig. 1, hot fluid at T_h enters the desorbing bed (Bed A) heat exchanger from the left. The temperature of the fluid decreases across a *thermal wavefront* as heat is transferred from the fluid to the adsorbent. The fluid leaves the right side of the bed at temperature T_{1+} which is slightly higher than the cycle's low temperature. The fluid is cooled to T_1 in the fluid cooler and then enters the adsorbing bed (Bed B) heat exchanger from the right. The temperature of the fluid increases across the thermal wavefront in the adsorbing bed as heat is transferred from the adsorbent to the fluid, thereby recovering both sensible heat and the heat of adsorption. The fluid leaves the left side of the bed at temperature T_{h-}, which is slightly lower than the cycle's high temperature. The fluid is heated to T_h in the fluid heater and then reenters the left side of the Bed A heat exchanger. Of the total heat required by the cycle, only the amount needed to raise the fluid from T_{h-} to T_h is provided in the fluid heater. As the cycle progresses, the temperature of the fluid leaving the desorbing bed (Bed A) increases. This leads to a decline in efficiency as more heat is rejected in the fluid cooler. When the exit temperature reaches the reversing temperature T_R, the flow direction is reversed and Bed A becomes the adsorbing bed, while Bed B becomes the desorbing bed.

Thus, each bed executes an intermittent cycle that can be divided into four phases. During the first phase, *pressurization,* the heated adsorbent releases vapor, causing the bed pressure to rise. The *desorption* phase begins when the bed pressure exceeds the condenser pressure and refrigerant begins to flow out of the bed. After the heat transfer fluid flow direction is reversed, the cooled adsorbent captures vapor, causing the bed pressure to decrease during the *depressurization* phase. Finally, the *adsorption* phase begins when the bed pressure falls below the evaporator pressure and refrigerant begins to flow into the bed.

Contributed by the Advanced Energy Systems Division for publication in the JOURNAL OF ENERGY RESOURCES TECHNOLOGY. Manuscript received by the AES Division, November 25, 1997; revised manuscript received October 3, 1998. Associate Technical Editor: F. C. Chen.

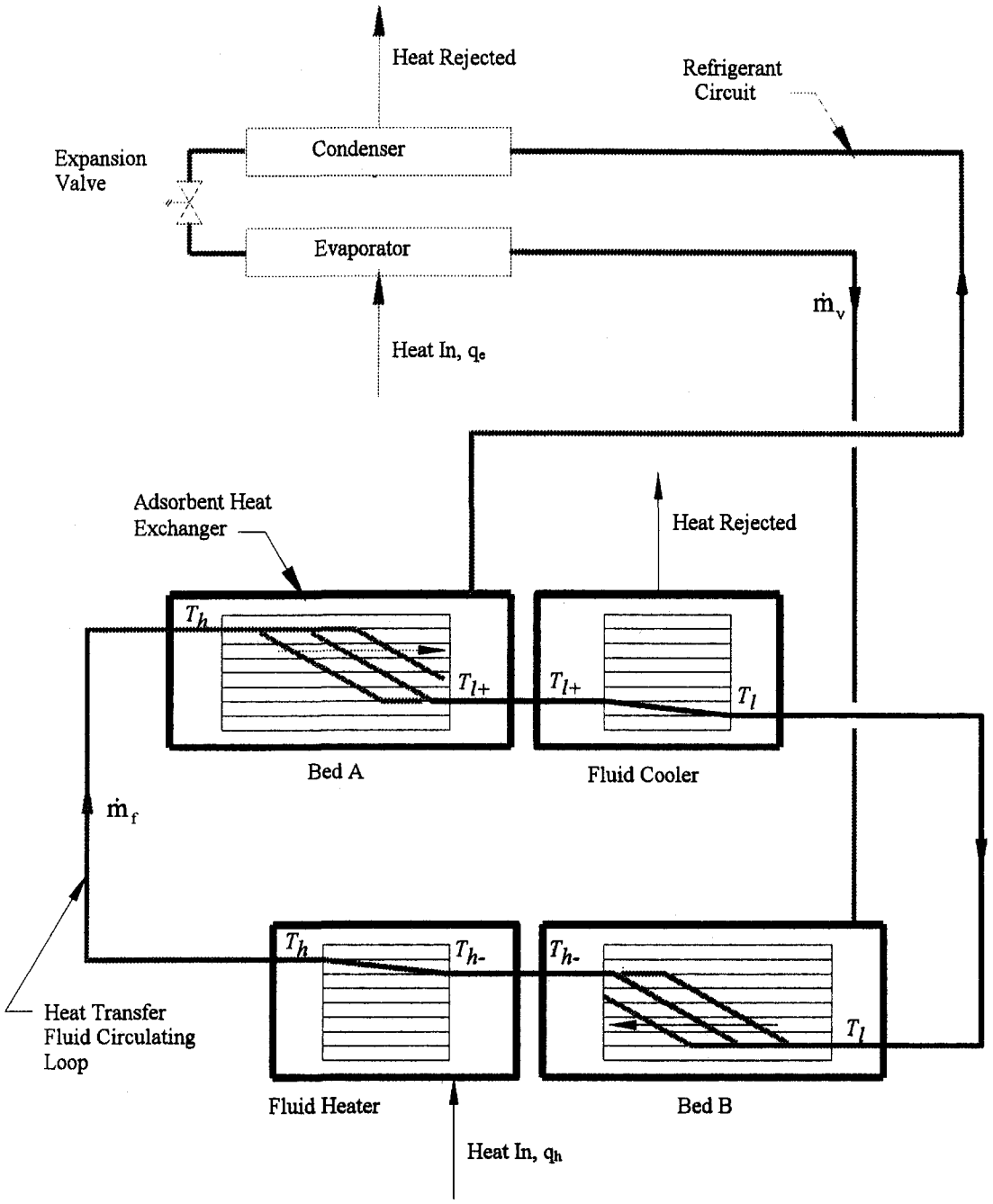

Fig. 1 Thermal wave heat pump system diagram

Nomenclature

b = tube wall thickness (m)
B = constant in vapor pressure curve correlation
c = specific heat (kJ/kg-K)
D = coefficient in Dubinin-Radusch-kovich equation (K^{-2})
Δh_{av} = integral enthalpy of adsorption (kJ/kg)
h = specific enthalpy (kJ/kg)
h_i = convective heat transfer coefficient at fluid/tube interface (W/m^2-K)
h_o = contact heat transfer coef. at tube/adsorbent interface (W/m^2-K)
k = thermal conductivity (W/m-K)
m = coefficient in vapor pressure curve correlation (K)
$\dot{m}$ = mass flow rate (kg/s)
P = pressure (kPa)
q = rate of heat transfer (W)
Q = heat transfer (kJ)
r = radial coordinate (m)
R = ideal gas constant (kPa-m^3/kg-K)
t = time (s)
u = specific internal energy (kJ/kg)
T = temperature (K)
V_{fl} = heat transfer fluid velocity (m/s)
$\mathbf{v}$ = vapor velocity vector (m/s)
v = component of vapor velocity vector (m/s)
z = axial coordinate (m)
ϵ = void volume
κ = permeability (m^2)
ρ = density (kg/m^3)
μ = dynamic viscosity (N-s/m^2)
ω = adsorption level (kg_a/kg_n)

Other types of regenerative cycles have been proposed, including thermal wave cycles using metal hydrides (Fateev and Rabinovich, 1997) and cascade cycles using adsorbent materials. The cascade cycle is similar in operation to the thermal wave cycle, except that the adsorbent heat exchangers are designed to yield a uniform temperature within each adsorbent bed. With this configuration, the heating and cooling operations are accomplished by separate circulating fluid loops. Heat recovery is accomplished intermittently by interconnecting the loops and "cascading" heat from one bed to the other. The system described by Douss et al. (1988), which uses water as a refrigerant and two zeolite adsorbent beds, is representative of a typical cascade design.

Cascade cycles allow greater flexibility in the design of the adsorbent heat exchangers and can achieve a higher utilization of the adsorbent. However, they require more complex piping and controls, impose longer delays between half-cycles, and do not recover heat as effectively as thermal wave cycles. The effectiveness of the heat recovery can be improved by increasing the number of adsorbent beds, but this comes at the expense of additional system complexity. Meunier found that in the limit of an infinite number of cascades, the efficiency of the cascade cycle approached 68 percent of the Carnot efficiency (Meunier, 1985).

For both the thermal wave cycle and the cascade cycle, the performance is strongly influenced by the heat and mass transfer properties of the adsorbent. A number of researchers have investigated techniques for improving the thermal conductivity of adsorbent materials. These techniques include the introduction of fins and metal matrices into the bed and the use of binders by themselves and with metal matrices (Guilleminot and Gurgel, 1990; Guilleminot et al., 1993; Basile et al., 1991, 1992; Cacciola et al., 1990, 1992; Groll, 1992). The use of binders and pressure forming to create a consolidated adsorbent is particularly attractive and researchers have reported significant increases in the bed thermal conductivity and in the heat transfer coefficient at the interface between the heat transfer tubes and the adsorbent. For example, Guilleminot et al. (1993) described a consolidated adsorbent with an embedded metal matrix that exhibited a thermal conductivity 100 times greater than that of a typical packed bed. However, these improvements come at the expense of a reduction in the permeability of the adsorbent. The reduced permeability can diminish performance by restricting the flow of refrigerant through the material. The net effect on the performance of a thermal wave heat pump can only be determined through the development of a heat pump model that incorporates the effects of both heat and mass transfer within the adsorbent material.

Several thermal wave heat pump models have been proposed, ranging from simple thermodynamic models to more complex models that also include heat transfer effects. Early heat pump models assumed temperature profiles within the adsorbent heat exchanger and calculated performance strictly from a thermodynamic analysis (Shelton et al., 1990; Härkönen and Aittomäki, 1992). Subsequent analyses incorporated a one-dimensional heat transfer model in which the adsorbent temperature gradient normal to the heat transfer tubes was assumed small compared to the temperature gradient along the axis of the tube (Tchernev and Emerson, 1988; Hajji and Worek, 1991; Fuller et al., 1994). In general, however, the normal gradients are significant and more advanced two-dimensional models were developed to account for these effects (Miles and Shelton, 1991; Härkönen and Aittomäki, 1991; Zheng et al., 1995). Amar et al. (1992) developed a two-dimensional heat and mass transfer model that considered the effects of thermal conductivity and permeability on temperature and pressure gradients within an adsorbent bed. However, their model was not incorporated into a system model, and, therefore, was not able to assess the effects of conductivity and permeability on performance.

The evaluation of the effects of conductivity and permeability on thermal wave cycle performance requires the development of a heat and mass transfer model that is integrated into a system model. This integrated model can then be used to evaluate performance for the range of adsorbent material properties identified by Guilleminot et al. (1993). This analysis is complicated by the fact that heat pump performance is a function, not only of material properties, but also of a variety of design and operating variables. In order to achieve a meaningful comparison, the performance for each set of adsorbent material properties must be evaluated at the optimum design and operating conditions for that property set. The following sections describe the heat pump model, the application of the model, and the results of the property evaluation.

Model Development

System Performance Model. A model of the thermal wave heat pump that calculates the capacity and the coefficient of performance (COP) can be developed by applying the principle of conservation of energy to the components of the heat pump illustrated in Fig. 1. For the evaporator, this yields

$$q_e = \dot{m}_v(h_g(P_e) - h_f(P_e)) \tag{1}$$

Since the refrigerant flow rate varies from zero during the pressurization phase to a maximum during the desorption phase, it is more meaningful to describe the performance in terms of the cooling rate averaged over the half-cycle

$$\bar{q}_e = (h_g(P_e) - h_f(P_e))\frac{1}{t_{1/2}}\int_0^{t_{1/2}} \dot{m}_v dt \tag{2}$$

In order to achieve this rate of cooling, energy must be supplied at the fluid heater. Applying conservation of energy to the fluid heater and averaging over a half-cycle yields the average rate of heat addition

$$\bar{q}_h = \frac{1}{t_{1/2}}\int_0^{t_{1/2}} \dot{m}_{\mathrm{fl}} c_{\mathrm{fl}}(T_h - T_{\mathrm{fl,exit}}(t))dt \tag{3}$$

The cooling coefficient of performance COP_c for the cycle is calculated as the average cooling rate divided by the average rate of heat addition

$$\mathrm{COP}_c = \frac{\bar{q}_e}{\bar{q}_h} \tag{4}$$

The refrigerant mass flow rate required to calculate $\bar{q}_e$ and the fluid heater exit temperature required to calculate $\bar{q}_h$ must

Nomenclature (cont.)

Subscripts

a = adsorbate
c = condenser
e = evaporator
f = saturated liquid
fl = heat transfer fluid
g = saturated vapor
h = high
l = low
n = adsorbent
p = pore
s = saturation
t = tube
v = refrigerant vapor
1/2 = half-cycle

Superscripts

$\hat{}$ = nondimensional value
$\bar{}$ = average value

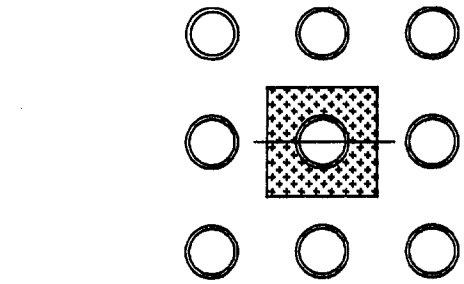

(a) Actual adsorbent heat exchanger geometry

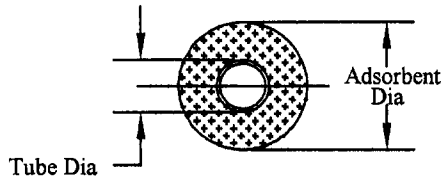

(b) Model Adsorbent heat exchanger geometry

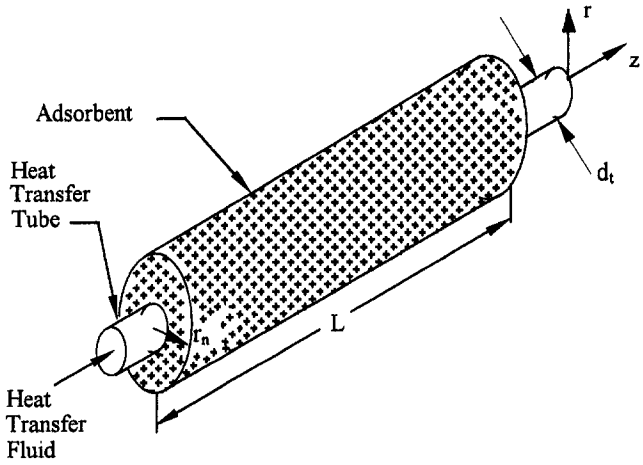

(c) Typical adsorbent heat exchanger element

Fig. 2 Adsorbent heat exchanger geometry

be found by solving the coupled conservation equations describing heat and mass transfer in the adsorbent heat exchangers.

Heat and Mass Transfer Model. The fluid exit temperature and mass flow rate of refrigerant can be determined by applying the equations of conservation of mass, momentum, and energy in the adsorbent heat exchangers. For this analysis, each adsorbent bed heat exchanger is assumed to consist of an array of cylindrical heat transfer tubes surrounded by adsorbent material. Each tube in the heat exchanger is approximated by the element shown in Fig. 2 where the adsorbent diameter is selected to enclose the same area of adsorbent as the square area in Fig. 2(*a*). This approximation allows the analysis to be accomplished in two dimensions—axial and radial.

The adsorbent material is treated as a continuum with a representative elementary volume as depicted in Fig. 3. This volume is much larger than the individual adsorbent particles, but much smaller than the overall system dimensions. Likewise, the surface area of the elementary volume is much larger than the individual pore and solid grain cross sections. This representative volume contains three phases defined as:

1 adsorbent—the microporous material in which adsorption occurs;
2 adsorbate—the sorbate (refrigerant) that is captured within the adsorbent;
3 vapor—the sorbate that exists as a gas and that is free to move within the void space surrounding the adsorbent particles.

These three phases are assumed to exist at the same temperature, T_n. The fraction of the bed that is not occupied by adsorbent particles is called the void fraction and is represented by the symbol ϵ. The void space is occupied by the vapor phase, which is assumed to behave as an ideal gas with constant specific heat. The remaining volume fraction, $(1 - \epsilon)$, is occupied by the adsorbent and adsorbate, both of which are assumed to be stationary. The mass of adsorbate contained within the control volume varies and is equal to the product of the adsorbent density, ρ_n, and the adsorption level, ω, which is defined as the ratio of the mass of adsorbate to the mass of adsorbent. The adsorption level is a function of both the pressure and temperature existing within the control volume. This function is given by an adsorption equilibrium relation that is specific to the adsorbent/sorbate combination.

The analysis of the heat pump system is simplified by employing the following assumptions:

(*a*) constant magnitude for the heat transfer fluid flow rate;
(*b*) constant thermal conductivities for all materials;
(*c*) constant specific heats for all materials;
(*d*) constant densities for solids and liquids;
(*e*) refrigerant vapor behaves as an ideal gas;
(*f*) adsorbate phase behaves as a liquid with a very small specific volume;
(*g*) stationary adsorbent and adsorbate phases;
(*h*) local thermal equilibrium between the adsorbent, adsorbate, and vapor phases;
(*i*) local adsorption equilibrium.

Subject to these assumptions, conservation of energy for the circulating fluid yields

$$\pi r_t^2 \rho_{fl} c_{fl} \frac{\partial T_{fl}}{\partial t} - \pi r_t^2 k_{fl} \frac{\partial}{\partial z}\left(\frac{\partial T_{fl}}{\partial z}\right) + \begin{bmatrix} + \\ - \end{bmatrix} \pi r_t^2 \rho_{fl} c_{fl} V_{fl} \frac{\partial T_{fl}}{\partial z} + 2\pi r_t h_i (T_{fl} - T_t) = 0 \quad (5)$$

where the sign of the third term is positive during pressurization/desorption and negative during depressurization/adsorption.

Applying conservation of energy to the tube wall and assuming that the tube cross-sectional area can be approximated as $2\pi r_t b$, where r_t is the tube radius and b the wall thickness yields

$$2\pi r_t b \rho_t c_t \frac{\partial T_t}{\partial t} - 2\pi r_t b k_t \frac{\partial}{\partial z}\left(\frac{\partial T_t}{\partial z}\right) - 2\pi r_t h_i (T_{fl} - T_t) + 2\pi r_t h_o (T_t - T_n(r_t, z)) = 0 \quad (6)$$

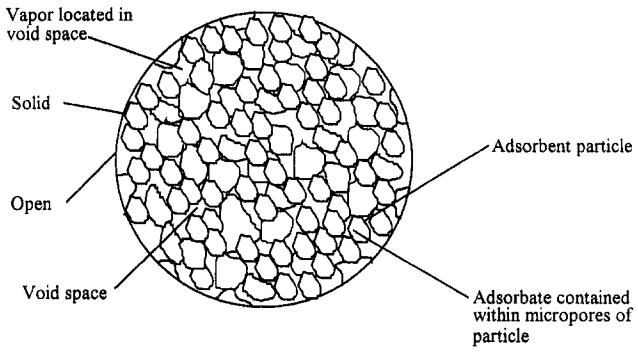

Fig. 3 Representative adsorbent volume

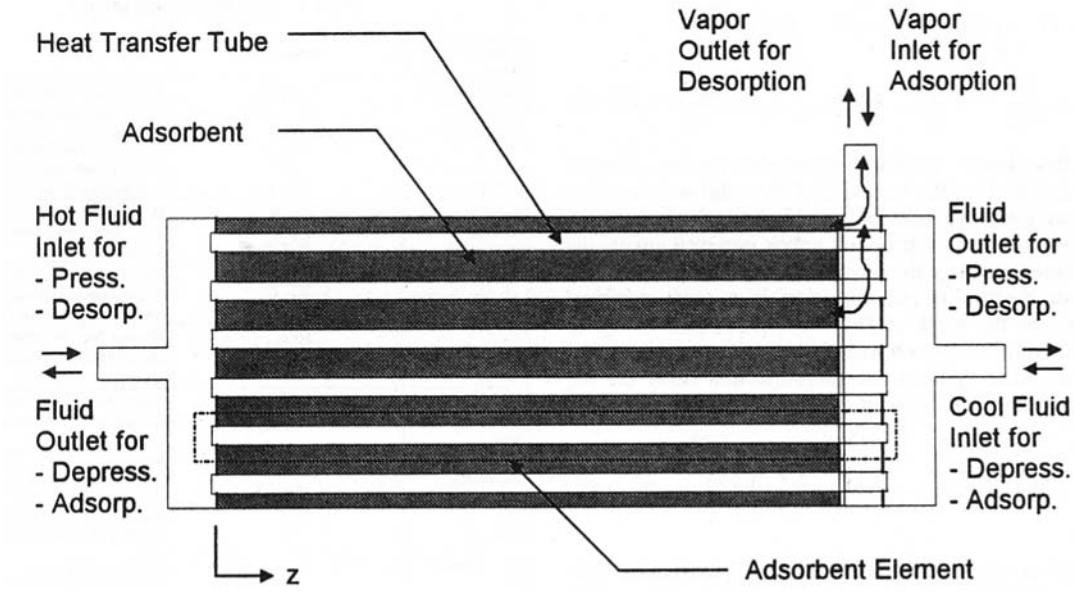

Fig. 4 Adsorbent heat exchanger configuration

In Eqs. (5) and (6), radial temperature gradients are negligible relative to axial gradients, and both equations are one-dimensional, unsteady equations coupled to each other at the tube wall. The tube wall equation is also coupled to the adsorbent at the tube/adsorbent interface.

The conservation equations for mass, momentum and energy within the adsorbent material are two-dimensional, unsteady equations, coupled to each other and coupled to the tube wall energy equation at the inner boundary of the adsorbent. These equations can be simplified by considering the flow configuration of the adsorbent heat exchanger as illustrated in Fig. 4. With this configuration, the refrigerant vapor flow is axial and the outer perimeter of each annular adsorbent element is effectively closed to mass flow due to the influence of the adjacent elements. In addition, the inner boundary is closed to mass flow due to the presence of the impermeable tube wall. Therefore, radial mass flux is neglected and the conservation of mass equation can be averaged over the radial direction. Furthermore, if the radial mass flux is neglected, then the conservation of momentum equation must only be developed for the axial direction. The conservation of energy equation must still include both radial and axial effects since the temperature variations in both directions are significant.

The conservation of mass equation for the adsorbent bed is

$$\frac{\partial}{\partial t}(\epsilon\rho_v + (1-\epsilon)\rho_n\omega) + \nabla\cdot(\rho_v\mathbf{v}) = 0 \qquad (7)$$

In Eq. (7), the first time derivative term accounts for storage of refrigerant vapor within the void space of the material. The second time derivative term accounts for storage of refrigerant in the adsorbed phase. The flux term reflects the movement of vapor due to pressure-driven flow at the area averaged or Darcian velocity, $\mathbf{v}$. Neglecting radial mass flux terms and averaging the remaining variables over the radial direction yields

$$\frac{\partial}{\partial t}(\epsilon\overline{\rho}_v + (1-\epsilon)\rho_n\overline{\omega}) + \frac{\partial(\overline{\rho_v v_z})}{\partial z} = 0 \qquad (8)$$

where the overbars indicate radially averaged terms.

Since the radial mass flux is negligible, only the axial component of the momentum equation must be considered. Furthermore, an order of magnitude analysis for typical heat pump operating conditions indicates that bulk convective and viscous terms as well as unsteady terms in the momentum equation are relatively small when compared to the pore level viscous and inertial terms (Ellis, 1996). Therefore, the conservation of momentum equation represents a balance between the pressure gradient and the force per unit volume imposed by the porous adsorbent. The force imposed by a porous medium is a function of the flow velocity and can be determined from empirical correlations. Many of these expressions are based on the work of Ergun, who developed a correlation for pressure loss due to flow through a porous medium that includes both microscale viscous and inertial forces (Vafai and Tien, 1981). Using Ergun's approach, the pressure gradient and the velocity are related by

$$\frac{\partial P}{\partial z} = -\frac{\mu\overline{v}_z}{\kappa}(1 + C_E\mathbf{Re}_\kappa^{1/2}) \qquad (9a)$$

where

$$\mathbf{Re}_\kappa^{1/2} = \frac{\rho|\mathbf{v}|\kappa^{1/2}}{\mu} \qquad (9b)$$

$$C_E = 0.55 \text{ (Ward, 1964)} \qquad (9c)$$

The 1 in parentheses in Eq. (9a) accounts for the viscous, or Darcy's law, component of the friction. The second term in parentheses accounts for the turbulent component of friction and is significant at higher $\mathbf{Re}_\kappa^{1/2}$.

The final conservation equation, conservation of energy for the adsorbent, can be written

$$\frac{\partial}{\partial t}(\epsilon\rho_v u_v + (1-\epsilon)\rho_n u_n + (1-\epsilon)\rho_n\omega u_a) + \frac{\partial(h_v\overline{\rho_v v_z})}{\partial z} - \nabla\cdot(k_n\nabla T_n) = 0 \qquad (10)$$

In this expression, the components of the first term represent storage of energy in the vapor, adsorbent, and adsorbate phases, respectively. The second term represents the convection of energy with the refrigerant vapor, and the third term represents conduction within the adsorbent. Incorporating Eq. (8), applying the assumptions presented previously, and rearranging yields

$$\epsilon\rho_v c_{p,v}\frac{\partial T_n}{\partial t} + (1-\epsilon)\rho_n c_n\frac{\partial T_n}{\partial t} + (1-\epsilon)\rho_n\omega\frac{\partial u_a}{\partial t}$$

$$-(1-\epsilon)\rho_n h_{av}\frac{\partial\omega}{\partial t} - \epsilon\frac{\partial P}{\partial t} - k_n\nabla^2 T_n + c_{p,v}\overline{\rho_v v_z}\frac{\partial T_n}{\partial z} = 0 \quad (11)$$

Property Relations. In order to complete the set of equations required to analyze the behavior of the solid sorption heat pump, property relations must be specified for the adsorption equilibrium behavior, the refrigerant vapor pressure curve, the enthalpy of adsorption, and the internal energy of the adsorbate.

The Dubinin-Raduschkovich equation is a semi-empirical equation based on the work of Dubinin (1967) that describes the adsorption equilibrium behavior for a variety of adsorbent/sorbate systems. The systems considered in this study are described using a modified form of the Dubinin-Raduschkovich equation

$$\omega = \omega_0 \exp\left(-DT^2\left(\ln\left(\frac{P_s}{P}\right)\right)^2\right) \quad (12)$$

where ω_0 and D are experimentally determined parameters. Values for these parameters for ammonia interacting with various adsorbents can be found in the literature (Critoph and Turner, 1988).

Refrigerant vapor pressure data can be fit to an equation of the form

$$\ln P_s = B - m\frac{1}{T} \quad (13)$$

The differential enthalpy of adsorption can be determined from the adsorption equilibrium expression and the refrigerant vapor pressure parameters. Within the typical range of adsorption levels, $0.05 \le \omega/\omega_0 \le 0.95$, the differential enthalpy of adsorption can be approximated by the linear expression (Ellis, 1996)

$$h_{av}(\omega) = \left[Rm + \frac{1.58R}{D^{1/2}}\right] - \left[\frac{1.42R}{D^{1/2}\omega_0}\right]\omega \quad (14)$$

Assuming that the specific volume of the adsorbed phase is small, the adsorbed phase internal energy is approximately equal to the adsorbed phase enthalpy, which can be determined with respect to a reference enthalpy in the vapor phase

$$u_a \approx h_a = h_{ref} + c_{p,v}(T - T_{ref}) - \Delta\bar{h}_{av} \quad (15)$$

where the integral enthalpy of adsorption, $\Delta\bar{h}_{av}$, is the mean difference between the adsorbed phase enthalpy and the vapor phase enthalpy. The integral enthalpy of adsorption is determined by averaging the differential enthalpy of adsorption from an adsorption level of 0 to the adsorption level at the state of interest. Applying this approach yields

$$u_a \cong h_a = h_{ref} + c_{p,v}(T - T_{ref}) - \left[Rm + \frac{1.58R}{D^{1/2}}\right] + \frac{1}{2}\left[\frac{1.42R}{D^{1/2}\omega_0}\right]\omega \quad (16)$$

Nondimensional Governing Equations. The governing equations for heat and mass transfer in the adsorbent heat exchanger can be written in nondimensional form by introducing the following variables (Ellis, 1996):

$$\hat{z} = \frac{z}{L} \quad \hat{r} = \frac{r}{r_n} \quad \hat{P} = \frac{P}{P_c} \quad (17a, b, c)$$

$$\hat{T}_f = \frac{T_f}{T_h} \quad \hat{T}_t = \frac{T_t}{T_h} \quad \hat{T}_n = \frac{T_n}{T_h} \quad (17d, e, f)$$

Table 1 Nondimensional groups

Symbol *Name*	Definition	Interpretation
A *ND Vapor Specific Volume*	$\frac{1-\varepsilon}{\varepsilon}\frac{\rho_n\omega_0}{\rho_v^s}$	Ratio of the vapor specific volume to the adsorbate specific volume.
$\mathbf{Bi}_c$ *Contact Biot number*	$\frac{h_o}{h_i}$	Ratio of tube/adsorbent contact heat transfer coefficient to the convective coefficient (Zheng et al., 1995).
$\mathbf{C}_{av}$ *ND Heat of Adsorption*	$\frac{\rho_n\omega_0 h_{av}^s}{\rho_n c_n T_H}$	Ratio of the thermal capacitance associated with adsorption to that of the adsorbent.
$\mathbf{C}_{tf}$ *ND Tube Thermal Capacitance*	$\frac{2b\rho_t c_t}{r_i\rho_f c_f}$	Ratio of the heat transfer tube thermal capacitance to the heat transfer fluid thermal capacitance.
$\mathbf{C}_p$ *ND Vapor Specific Heat*	$\frac{\varepsilon\rho_v^s c_{p,v}}{(1-\varepsilon)\rho_n c_n}$	Ratio of the vapor thermal capacitance to the adsorbent thermal capacitance.
$\mathbf{C}_{pr}$ *ND Compression Work*	$\frac{\varepsilon P_c}{(1-\varepsilon)\rho_n c_n T_h}$	Ratio of the compression work to the adsorbent thermal capacitance.
Fo *Fourier No.*	$\frac{k_n t^s}{(1-\varepsilon)\rho_n c_n r_n^2}$	Ratio of the system time scale to the time scale for radial conduction.
$\mathbf{H}_0$ *Time ratio*	$\frac{V_f t^s}{L}$	Ratio of the system time to the time for fluid to traverse the length of the tube.
$\mathbf{N}_l$ *Aspect ratio*	$\frac{L}{r_n}$	Ratio of adsorbent length to the adsorbent radius.
NTU *Number of transfer units*	$\frac{2\pi r_i L h_i}{\pi r_i^2 V_f\rho_f c_f}$	Ratio of the heat transfer at the tube wall to the advection of energy in the fluid.
Pe *Peclet No.*	$\frac{V_f L}{k_f/\rho_f c_f}$	Ratio of axial advection to axial conduction in the fluid.
$\mathbf{\Omega}_t$ *Non-dimensional tube resistance*	$\frac{r_i k_f}{2bk_t}$	Ratio of the thermal resistance of the tube to the thermal resistance of the heat transfer fluid.

$$\hat{\rho}_v = \frac{\rho_v}{P_c/RT_h} \quad \hat{\omega} = \frac{\omega}{\omega_0} \quad \hat{h}_{av} = \frac{h_{av}}{h_{av,\omega\to 0}} \quad (17g, h, i)$$

$$\hat{v}_z = \frac{\overline{v}_z}{\left(\frac{r_i^2 V_f\rho_f c_f}{r_n^2\rho_n c_n}\cdot\frac{\rho_n\omega_0}{P_c/RT_h}\right)} \quad \hat{t} = \frac{t}{\left(\frac{(1-\epsilon)r_n^2 L\rho_n c_n}{r_i^2 V_f\rho_f c_f}\right)} \quad (17j, k)$$

Expressing Eqs. (5) and (6) in terms of these variables and dividing each equation by the heat transfer rate scale, $\dot{Q}^s$, where

$$\dot{Q}^s = \pi r_i^2 V_f\rho_f c_f T_h \quad (18)$$

yields

$$\frac{1}{\mathbf{H}_0}\frac{\partial\hat{T}_f}{\partial\hat{t}} - \frac{1}{\mathbf{Pe}}\frac{\partial^2\hat{T}_f}{\partial\hat{z}^2} + \begin{bmatrix}+\\-\end{bmatrix}\frac{\partial\hat{T}_f}{\partial\hat{z}} + \mathbf{NTU}(\hat{T}_f - \hat{T}_t) = 0 \quad (19)$$

and:

$$\frac{\mathbf{C}_{tf}}{\mathbf{H}_0}\frac{\partial\hat{T}_t}{\partial\hat{t}} - \frac{1}{\mathbf{\Omega}_t\mathbf{Pe}}\frac{\partial^2\hat{T}_t}{\partial\hat{z}^2} - \mathbf{NTU}(\hat{T}_f - \hat{T}_t) + \mathbf{NTU}\cdot\mathbf{Bi}_c(\hat{T}_t - \hat{T}_n(\hat{r}, \hat{z})) = 0 \quad (20)$$

where the nondimensional groups are defined in Table 1.

Writing Eq. (8) in terms of the nondimensional variables and dividing by the resulting coefficient of the first term yields the following nondimensional equation for conservation of mass in the adsorbent bed:

$$\frac{\partial\overline{\rho}_v}{\partial\hat{t}} + \mathbf{A}\frac{\partial\overline{\omega}}{\partial\hat{t}} + \mathbf{A}\frac{\partial(\overline{\hat{\rho}_v\hat{v}_z})}{\partial\hat{z}} = 0 \quad (21)$$

The conservation of momentum equation, Eq. (11), can be expressed in nondimensional form as

Table 2 Boundary conditions

Fluid temperature:	
Pressurization and desorption:	$\hat{T}_f(0) = \hat{T}_h \qquad \frac{\partial \hat{T}_f}{\partial \hat{z}}(1) = 0$
Depressurization and adsorption:	$\frac{\partial \hat{T}_f}{\partial \hat{z}}(0) = 0 \qquad \hat{T}_f(1) = \hat{T}_l$
Tube temperature (all phases):	$\frac{\partial \hat{T}_t}{\partial \hat{z}}(0) = \frac{\partial \hat{T}_t}{\partial \hat{z}}(1) = 0$
Adsorbent temperature (all phases):	$\frac{\partial \hat{T}_n}{\partial \hat{r}}(\hat{r}_t, \hat{z}) = \frac{h_g r_n}{k_n}\left(T_f(\hat{z}) - T_n(\hat{r}_t, \hat{z})\right)$
	$\frac{\partial \hat{T}_n}{\partial \hat{r}}(1, \hat{z}) = \frac{\partial \hat{T}_n}{\partial \hat{z}}(\hat{r}, 0) = \frac{\partial \hat{T}_n}{\partial \hat{z}}(\hat{r}, 1) = 0$
Pressure:	
Pressurization and depressurization:	$\frac{\partial \hat{P}}{\partial \hat{z}}(1) = 0$
Desorption:	$\hat{P}(1) = \hat{P}_c$
Adsorption:	$\hat{P}(1) = \hat{P}_e$

$$\hat{v}_z = -F_{\mathrm{Er}}(\mathbf{Re}_{\kappa^{1/2}}) \frac{\partial \hat{P}}{\partial \hat{z}} \tag{22a}$$

where the function F_{Er} is defined as

$$F_{\mathrm{Er}}(\mathbf{Re}_{\kappa^{1/2}}) = \frac{\kappa P^*}{\mu_v(1 + 0.55\mathbf{Re}_{\kappa^{1/2}})v^s L} \tag{22b}$$

with P^* representing the maximum pressure differential available for driving vapor flow. As defined by Eq. (22*b*), F_{Er}, is a measure of the pressure available for driving vapor flow relative to the pore level viscous and inertial forces. A high value of this function would indicate that the pressure differential is relatively high and that the sorption process is less likely to be limited by vapor flow restrictions.

Finally, the conservation of energy equation in the adsorbent bed, Eq. (11), can be expressed in nondimensional form by introducing the variables from Eqs. (17) and dividing by the coefficient of the adsorbent sensible heat storage term to get

$$\mathbf{C}_p \frac{\partial \hat{T}_n}{\partial \hat{t}} + \frac{\partial \hat{T}_n}{\partial \hat{t}} + \mathbf{C}_{\mathrm{av}}\hat{\omega} \frac{\partial}{\partial \hat{t}}\left(\frac{c_{p,v}}{h^s_{\mathrm{av}}} \hat{T}_n + \frac{0.71R}{h^s_{\mathrm{av}} D^{1/2}} \hat{\omega}\right)$$

$$- \mathbf{C}_{\mathrm{av}}\left(1 - \frac{1.42R}{h^s_{\mathrm{av}} D^{1/2}} \hat{\omega}\right) \frac{\partial \hat{\omega}}{\partial \hat{t}} - \mathbf{C}_{pr} \frac{\partial \hat{P}}{\partial \hat{t}} - \mathbf{Fo} \frac{1}{\hat{r}} \frac{\partial}{\partial \hat{r}}\left(\hat{r} \frac{\partial \hat{T}_n}{\partial \hat{r}}\right)$$

$$- \frac{\mathbf{Fo}}{\mathbf{N}_1^2} \frac{\partial^2 \hat{T}_n}{\partial \hat{z}^2} + \mathbf{C}_p \mathbf{A} \hat{\rho}_v \hat{v}_z \frac{\partial \hat{T}_n}{\partial \hat{z}} = 0 \tag{23}$$

Boundary Conditions. The boundary conditions associated with Eqs. (19) to (23) vary with the phase of the heat pump cycle. During the pressurization phase, the adsorbent heat exchanger is closed to vapor flow and the temperature of the fluid entering the heat exchanger at the left boundary is equal to the cycle high temperature. Once the pressure in the adsorbent reaches the condenser pressure, P_c, the right boundary of the adsorbent is opened to vapor flow initiating the desorption phase. During this phase, the fluid entering from the left remains at T_h, and the pressure of the vapor at the right end of the adsorbent is maintained at P_c. When the temperature of the fluid leaving the right end of the heat exchanger exceeds the reversing criterion, T_R, the direction of flow is reversed and the system begins the depressurization phase. During this phase, the adsorbent heat exchanger is closed to vapor flow and the fluid entering the right end of the tube is maintained at the cycle low temperature, T_l. Once the pressure in the adsorbent reaches the evaporator pressure, P_e, the left boundary of the adsorbent is opened to vapor flow, initiating the adsorption phase. During this phase, the fluid entering from the right remains at T_l, and the pressure of the vapor at the right end of the adsorbent is maintained at P_e. During all phases, the axial and outer radial boundaries of the adsorbent and the axial boundaries of the tube are assumed to be insulated. At the inner radial boundary of the adsorbent, conduction at the adsorbent boundary must be equal to the heat transfer across the contact resistance at the tube/adsorbent interface. These conditions are summarized in Table 2.

Initial Conditions. The heat pump cycle begins with the fluid, tube, and adsorbent at a uniform temperature equal to the cycle low temperature, T_l. The adsorbent pressure is also uniform and is equal to the evaporator pressure P_e. The heat pump then executes the four phases of the cycle. The temperature and pressure distributions that exist at the conclusion of the first cycle become the initial temperature and pressure distributions for the second cycle. After a number of cycles, usually 3–10, the system reaches a steady condition such that the final distributions of temperature and pressure at the conclusion of the cycle are approximately equal to the initial conditions that existed at the start of the cycle. Once the system reaches this steady state, the system performance remains constant through any additional cycles.

Numerical Analysis

The set of conservation equations represented by Eqs. (19) to (23) along with the boundary conditions listed in Table 2 and the property relations can be solved to yield the refrigerant mass flow rate and the fluid temperature entering the fluid heater as functions of time. These quantities can then be integrated in accordance with Eqs. (2) and (3) to determine system capacity and COP.

The set of equations consisting of the conservation equations and property relations is nonlinear and must be solved using numerical techniques. The solution was accomplished using a finite difference technique that is implicit in time to improve the numerical stability. First-order spatial derivatives that do not involve convection were replaced by second-order accurate central difference approximations. First derivatives that do appear in convective terms were discretized using a first-order accurate upwind approximation to minimize numerical instability (Hall and Porsching, 1990). Second-order spatial derivatives were replaced by second-order accurate central difference approximations. The resulting set of nonlinear algebraic equations was solved at each time step using an iterative approach as follows:

1 Solve the finite difference forms of the energy equations, Eqs. (19), (20), and (23), for the fluid, tube, and adsorbent temperatures using a line iterative approach based on values of $\hat{P}(\hat{z})$ and $\hat{\omega}(\hat{r}, \hat{z})$ from the most recent iteration.
2 Update $\hat{\omega}(\hat{r}, \hat{z})$ based on the new adsorbent temperatures.
3 Solve the finite difference forms of Eqs. (21) and (22) for the axial pressure distribution, $\hat{P}(\hat{z})$, in the adsorbent assuming $\hat{T}_n(\hat{r}, \hat{z})$ and $\hat{\omega}(\hat{r}, \hat{z})$ are known from the most recent iteration.
4 Update $\hat{\omega}(\hat{r}, \hat{z})$ based on the new adsorbent pressures.
5 Repeat steps 1 to 4 to convergence and then advance to the next time step.

Table 3 Base case parameters

Application Temperatures:	
Comfort cooling in summer:	$T_e = 7°C$, $T_c = T_l = 41°C$
Gas fired heat source:	$T_h = 230°C$
Refrigerant:	Ammonia
Adsorbent:	Activated carbon AX21 (Critoph and Turner, 1988)
Heat transfer tubes:	Steel tubes, 4m L × 3mm D× 0.6mm wall
Heat transfer fluid:	$\rho_f = 914$ kg/m3; $c_f = 1.93$ kJ/kg°C; $k_f = 0.115$ W/m°C

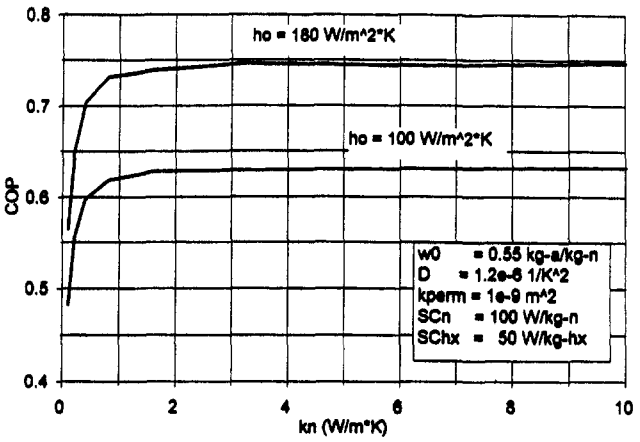

Fig. 5 Effect of adsorbent heat transfer properties on COP

Appropriate values for the temporal and spatial increments were determined by reducing the size of the increment until further changes did not affect the results. The numerical code was verified by applying it to simplified problems with published solutions, by utilizing test functions, and by comparison to limited experimental data (Ellis, 1996).

Results

As indicated by Eqs. (19) to (23), the performance of the thermal wave heat pump is a function of a number of parameters. In order to analyze the influence of thermal conductivity and permeability, a basis that specifies the remaining parameters must be established. The base case parameters assumed for this paper are indicated in Table 3. The application temperatures are based on comfort cooling applications during the summer months. The heat source temperature is representative of the temperatures utilized in prototype systems reported in the literature (Miles et al., 1992; Poyelle et al., 1996). Ammonia is chosen as the refrigerant because it has excellent refrigeration properties, adsorbs well on carbon, can be used at sub-freezing temperatures, and operates at a pressure high enough to facilitate vapor transport. The AX21 carbon exhibits a relatively high saturation sorption level and an equilibrium coefficient, D, that is very close to the optimum for the given application (Ellis, 1996). The dimensions of the heat transfer tube are of the same order of magnitude as those for a prototype thermal wave heat pump described by Miles and Shelton (1991). The fluid characteristics are also similar to those used in the prototype. These assumptions regarding the application, refrigerant, adsorbent, and heat transfer tube, establish values for the following variables:

$$\mathbf{A} = 113 \quad \Omega_t = 0.0083 \quad \mathbf{C}_{av} = 2.67 \quad (24a, b, c)$$

$$\mathbf{C}_{tf} = 1.89 \quad \mathbf{C}_p = 0.014 \quad \mathbf{C}_{pr} = 0.0028 \quad (24d, e, f)$$

In order to determine the remaining dimensionless variables, values must be specified for the design parameters of fluid velocity, adsorbent radius, and reversing criteria, and the material parameters of thermal conductivity, contact heat transfer coefficient, and permeability. Each of these parameters has a significant effect on performance and the effects are interrelated. For example, increased consolidation of the adsorbent improves not only the conductivity of the adsorbent, but also the contact heat transfer coefficient. Thermal properties may also be affected by the pressure within the adsorbent bed; however, the effect of pressure is less important in ammonia-based systems that operate at relatively high pressures and is neglected here. The effects of thermal conductivity, contact heat transfer coefficient, and permeability are evaluated as if they can be varied independently. This approach identifies the effect of each of these parameters on system performance. These results coupled with data from other research defining the relationship among adsorbent properties can be used to improve system design.

In order to evaluate the effects of thermal conductivity, contact heat transfer coefficient, and permeability, a multi-dimensional optimization technique was employed to adjust the design variables to obtain the "best performance" for a given set of these three material parameters. Best performance was defined as the highest cooling COP achievable subject to minimum capacity constraints of 100 W/kg-adsorbent and 50 W/kg-heat exchanger. The optimization technique that was employed was based on the multidimensional simplex method (Nelder and Mead, 1965; Press et al., 1992). Constraints were imposed through penalty functions as described by Pike (1986).

Results obtained using this approach are illustrated in Fig. 5. This figure indicates the influence of the thermal conductivity for different values of the contact heat transfer coefficient and for a permeability of 1×10^{-9} m^2, which corresponds to the permeability of a granular bed. Values for the thermal conductivity and contact heat transfer coefficient were chosen to span the range of values reported by Guilleminot et al. (1993). As this figure indicates, increasing conductivity improves performance up to a value of approximately 1 W/m-K. Further increases in the conductivity yield little improvement in COP. This figure also indicates that COP can be improved by increasing the contact heat transfer coefficient. These results suggest that for values of thermal conductivity in excess of 1 W/m-K, the conductive resistance of the adsorbent is relatively small compared to the resistance imposed by the fluid film and the adsorbent/tube contact.

The results depicted in Fig. 5 were obtained assuming that the improvements in conductivity and contact heat transfer coefficient could be achieved without decreasing the permeability. The maximum COP predicted for these idealized conditions was 0.75. However, the consolidation process that produces the improvement in thermal properties also reduces the conductivity (Guilleminot et al., 1993). The effect of this reduction in permeability on performance is indicated in Fig. 6. Values of COP were obtained by varying permeability while maintaining a contact heat transfer coefficient of 180 W/m^2-K and a permeability of 10 W/m-K. These results indicate that even with enhanced thermal properties, values of permeability below 1.5×10^{-11} m^2 result in performance that is less than that achieved by typical granular materials with their lower thermal properties. The high conductivity materials reported by Guilleminot exhibited permeability values as low as 10^{-13} m^2. Clearly materials with values of permeability this low could not produce enhanced performance. However, Poyelle notes that arteries may be pro-

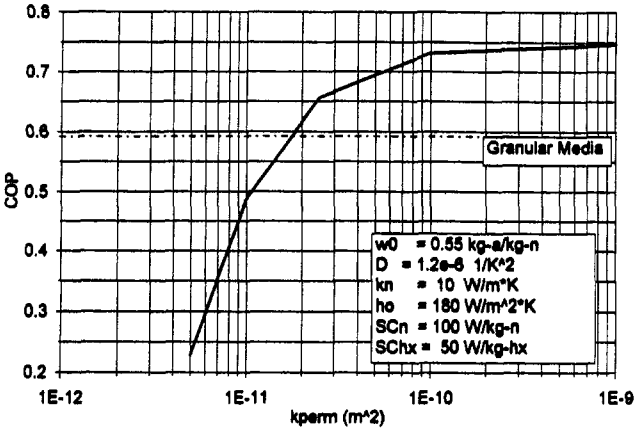

Fig. 6 Effect of adsorbent permeability on COP

vided in these materials to increase the effective permeability to approximately 6.1×10^{-9} m^2 (Poyelle et al., 1996). Materials combining these higher effective values for permeability with enhanced thermal properties could produce significant improvements in performance.

Conclusions

The model developed in this study incorporates both the thermodynamic effects and the heat and mass effects occurring within the thermal wave heat pump system. The resulting model is capable of assessing the influence of a variety of parameters on heat pump performance. This study has focused on the influence of adsorbent thermal conductivity and permeability. The results indicate that for the base case considered here, improvements in thermal conductivity up to 1 W/m-K can lead to higher performance provided the permeability remains greater than 1.5×10^{-9} m^2. When the thermal conductivity exceeds 1 W/m-K, the resistance of the adsorbent becomes small relative to other elements of the overall resistance. Consequently, further increases in conductivity have a relatively small effect on performance. This study also indicates that if the permeability is less than 1.5×10^{-9} m^2, the performance of the heat pump is reduced below that which can be obtained by low-conductivity/high-permeability granular materials. The modeling techniques and results described here can provide assistance for ongoing research into the development of adsorbent materials with enhanced thermal properties.

References

Amar, N. B., Sun, L. M., and Meunier, F., 1992, "Pressure and Thermal Fronts Propagation in Adsorbers," *Solid Sorption Refrigeration Symposium,* International Institute of Refrigeration, Paris, France, pp. 64–73.

Basile, A., Cacciola, G., Colella, C., Mercadante, L., and Pansini, M., 1992, "Thermal Conductivity of Natural Zeolite-PTFE Composites," *Heat Recovery Systems & CHP,* Vol. 12(6), 497–503.

Basile, A., Cacciola, G., and Mercadante, L., 1991, "Physico-Chemical Study on Different Types of Carbon to be Applied in Refrigeration Adsorption Systems," 18th International Congress of Refrigeration, Montreal, Quebec, Canada.

Cacciola, G., Cammarata, G., Fichera, A., and Restuccia, G., 1992, "Advances on Innovative Heat Exchangers in Adsorption Heat Pumps," *Solid Sorption Refrigeration Symposium,* International Institute of Refrigeration, Paris, France, pp. 221–226.

Cacciola, G., Restuccia, G., Mirzain, H., and Giordano, N. 1990, "Pre-formed Zeolite Products to be Used in Adsorption Heat Pumps, Part 1: Methodology and Adsorption Measurements," *Adsorption Science & Technology,* Vol. 7(3), pp. 163–171.

Critoph, R. E., and Turner, H. L., 1988, "Activated Carbon-Ammonia Adsorption Cycle Heat Pumps," *Pompes á chaleur chimiques de hautes performance,* Perpignan.

Douss, N., Meunier, F., and Sun, L. M., 1988, "Predictive Model and Experimental Results for a Two Adsorber Solid Adsorption Heat Pump," *Industrial Engineering and Chemistry Research,* Vol. 27, pp. 310–316.

Dubinin, M. M., 1967, "Adsorption in Micropores," *Journal of Colloid and Interface Science,* Vol. 23, pp. 487–499.

Ellis, M. W., 1996, "An Evaluation of the Effects of Adsorbent Properties on the Performance of a Solid Sorption Heat Pump," Ph.D., Georgia Institute of Technology, Atlanta, GA.

Fateev, G. A., and Rabinovich, O. S., 1997, "Metal Hydride Heat Conversion on the Basis of Superadiabatic Combustion Waves in Porous Media," *International Journal of Hydrogen Energy,* Vol. 22(9), pp. 915–924.

Fuller, T. A., Wepfer, W. J., Shelton, S. V., and Ellis, M. W., 1994, "A Two Temperature Model of the Regenerative Solid-Vapor Heat Pump," ASME JOURNAL OF ENERGY RESOURCES TECHNOLOGY, Vol. 116, pp. 297–304.

Groll, M., 1992, "Reaction Beds for Dry Sorption Machines," *Solid Sorption Refrigeration Symposium,* International Institute of Refrigeration, Paris, France, pp. 207–214.

Guilleminot, J. J., Choisier, A., Chalfen, J. B., Nicolas, S., and Reymoney, J. L., 1993, "Heat Transfer Intensification in Fixed Bed Adsorbers," *Heat Recovery Systems & CHP,* Vol. 13(4), pp. 297–300.

Guilleminot, J. J., and Gurgel, J. M., 1990, "Heat Transfer Intensification in Adsorbent Beds of Adsorption Thermal Devices," *Solar Engineering 1990,* presented at the Twelfth Annual International Solar Energy Conference, Miami, FL, pp. 69–74.

Hajji, A., and Worek, W. M., 1991, "Simulation of a Regenerative, Closed-Cycle Adsorption Cooling/Heating System." *Energy,* 16(3), pp. 643–654.

Hall, C. A., and Porsching, T. A., 1990, *Numerical Analysis of Partial Differential Equations,* Prentice Hall, Englewood Cliffs, NJ.

Härkönen, M., and Aittomäki, A., 1991, "The Principle of Internal Regeneration as Applied to the Adsorption Heat Pump Process," *Heat Recovery Systems & CHP,* Vol. 11(4), pp. 239–248.

Härkönen, M., and Aittomäki, A., 1992, "Analytical Model for the Thermal Wave Adsorption Heat Pump Cycle," *Heat Recovery Systems & CHP,* Vol. 12(1), pp. 73–80.

Meunier, F., 1985, "Second Law Analysis of a Solid Adsorption Heat Pump Operating on Reversible Cascade Cycles: Application to the Zeolite—Water Pair," *Heat Recovery Systems,* Vol. 5(2), pp. 133–141.

Miles, D. J., Sanborn, D. M., Nowakowaski, G. A., and Shelton, S., 1992, "Gas-Fired Sorption Heat Pump Development," *Solid Sorption Refrigeration Symposium,* International Institute of Refrigeration, Paris, France, pp. 74–79.

Miles, D. J., and Shelton, S. V., 1991, "Coupled Heat Transfer and Thermodynamic Adsorption Heat Pump Analysis," ASME Advanced Energy Systems Division, *Heat Pump Design, Analysis, and Application,* Atlanta, GA, pp. 33–38.

Nelder, J. A., and Mead, R., 1965, "A Simplex Method for Function Minimization," *Computer Journal,* Vol. 7, pp. 308–313.

Pike, R. W., 1986, *Optimization for Engineering Systems,* Van Nostrand Reinhold Company Inc., New York, NY.

Poyelle, F., Guilleminot, J. J., and Meunier, F., 1996, "Analytical Study of a Gas-Fired Adsorptive Air-Conditioning System," *ASHRAE Transactions.* Vol. 102, No. 1, pp. 1128–1138.

Press, W. H., Teukolsky, S. A., Vetterling, W. T., and Flannery, B. P., 1992, *Numerical Recipes in FORTRAN: The Art of Scientific Programming,* Cambridge University Press, New York, NY.

Shelton, S. V., 1986, "Solid Adsorbent Heat Pump System," 4 610 148, U.S. Patent.

Shelton, S. V., Wepfer, W. J., and Miles, D. J., 1990, "Ramp Wave Analysis of the Solid/Vapor Heat Pump," ASME JOURNAL OF ENERGY RESOURCES TECHNOLOGY, Vol. 112, pp. 69–78.

Tchernev, D., and Emerson, D., 1988, "High-Efficiency Regenerative Zeolite Heat Pump," ASHRAE Annual Meeting publ.as *ASHRAE Transactions,* Ottawa, Canada, pp. 2024–2032.

Tchernev, D. I., 1987, "Heat Pump Energized by Low Grade Heat Source," 4 637 218, U.S. Patent.

Vafai, K., and Tien, C. L., 1981, "Boundary and Inertia Effects on Flow and Heat Transfer in Porous Media," *International Journal of Heat Mass Transfer,* Vol. 30, pp. 1391–1405.

Ward, J. C., 1964, "Turbulent Flow in Porous Media," *Journal of Hydrodynamics Division,* ASCE, 90(HY5), pp. 1–12.

Zheng, W., Worek, W. M., and Nowakowski, G., 1995, "Performance Optimization of Two-Bed Closed-Cycle Solid-Sorption Heat Pump Systems," *Heat and Mass Transfer,* Vol. 31, pp. 1–9.